journal

J. Am. Ceram. Soc., 91 [7] 2088–2097 (2008)
DOI: 10.1111/j.1551-2916.2008.02419.x

A Determination of Hydration Mechanisms for Tricalcium Silicate Using a Kinetic Cellular Automaton Model

Jeffrey W. Bullard†

Materials and Construction Research Division, National Institute of Standards and Technology, Gaithersburg, Maryland

Reaction mechanisms for the early stages of hydration of tricalcium silicate (Ca_3SiO_5) have not been agreed upon, although theories have appeared in the literature. In this paper, a mechanistic description is proposed that is consistent with a wide range of reported experimental observations, and which is supported quantitatively by simulations using HydratiCA, a new three-dimensional microstructure model of chemical kinetics. Rate processes are quantitatively modeled using probabilistic cellular automaton algorithms that are based on the principles of transition state theory. The model can test alternate assumptions about the reaction paths and rate-controlling steps, making it a kind of experimental tool for investigating kinetics and interpreting experimental observations. It is used here to show that hydration of Ca_3SiO_5 is most likely controlled by nucleation and growth of a compositionally variable calcium silicate hydrate solid, mediated at very early times by a transient, thermodynamically metastable solid that rapidly covers and sharply reduces the dissolution rate of Ca_3SiO_5. This proposed mechanism involves important elements of two leading theories of Ca_3SiO_5 hydration, neither of which alone has been able to capture the full range of experimental data when tested by the model.

I. Introduction

Tricalcium silicate (Ca_3SiO_5) is the primary constituent of a number of different types of cement, including ordinary Portland cement, white cement, and specialty cements used for oil-well applications.[1] Reaction between Ca_3SiO_5 and water is known to be the dominant cause of the setting and hardening of pastes made from these cements.[2] For this reason, Ca_3SiO_5 has often been used as a model material to study the hydration behavior of cement paste. Studies performed over the past 40 years have provided considerable information about the Ca_3SiO_5/water system, including phase chemistry and equilibria,[3–8] solid dissolution mechanisms,[9,10] overall rates of reaction,[11–16] and microstructure development.[12,17–23] However, a quantitative picture of the kinetics of this reaction sequence, consistent with the majority of experimental data, has not been agreed upon. Indeed, a consensus has not been reached even on the qualitative nature of the kinetic mechanisms, especially during the first several hours after mixing.

(1) Background

Hydration of Ca_3SiO_5 progresses through several different stages, across which the rate of reaction varies nonmonotonically by several orders of magnitude. These stages are shown in a generic way in Fig. 1, but each one can have different variable duration depending on the conditions of the experiment. Most researchers agree that changes in the rate-controlling step are responsible for these large but consistent variations in the rate, although there is less agreement about the actual nature of the rate-controlling steps, and what triggers the transition from one kinetic regime to another.[2,24]

Stage 1 is characterized by rapid dissolution of solid which begins immediately upon wetting. In the first 30 s or so, the pH of the surrounding solution increases from near 7 to about 12 to 12.5, the calcium ions in solution reach concentrations of 10–20 mmol/L, and the silicate concentration increases to between 50 and 200 μmol/L. Immediately afterward, however, the rate of dissolution decreases dramatically, and the system settles into a quiescent period (Stage 2, also called the induction period), which in pure systems can last for 1 or 2 hours and during which dissolution is extremely slow. At the beginning of Stage 2, the concentrations of the ions in solution are those already given. Assuming that the congruent dissociation reaction is

$$Ca_3SiO_5 + 3H_2O \rightleftharpoons 3Ca^{2+} + H_2SiO_4^{2-} + 4OH^-$$

then these concentrations correspond to an ion activity product of about 10^{-18}, which is 18 orders of magnitude less than the calculated equilibrium value of about 3.[25] This large discrepancy indicates that some kinetic inhibition of dissolution is quickly established, which signals the beginning of the induction period. Over the years, several hypotheses have been proposed for this inhibition. One theory is that a continuous layer of solid calcium silicate hydrate, no more than a few nanometers thick, rapidly forms on the surface of Ca_3SiO_5.[26,27] Although thin, this layer is assumed to have a low permeability and thus reduces the Ca_3SiO_5 dissolution rate by restricting its access to water. A second theory is that ions dissolving from Ca_3SiO_5 surfaces must be hydroxylated before detaching from the surface, and that this hydroxylation becomes rate-controlling.[9,10] A third and more recent hypothesis is that species in solution, such as calcium and hydroxyl ions, preferentially adsorb and poison the active dissolution sites on the Ca_3SiO_5 surfaces.[16,28]

Stage 3, the acceleration period, is characterized by an approximately exponential increase in the reaction rate, although the rate never is as great as in Stage 1. A reaction rate that increases exponentially with time is expected if the rate is controlled by growth of a solid, since the area available for growth increases with the solid volume.[29] This behavior, together with other experimental evidence, strongly indicates that the growth of a calcium silicate hydrate solid is the rate-controlling mechanism in Stage 3.[2] We will denote this solid hydrate as C–S–H‡ and, to avoid confusion, the hypothesized metastable hydrate mentioned previously will be denoted as C–S–H(m).

Stage 4 is characterized by a gradual decrease in the hydration rate. Experimental evidence suggests that the decelerating rate is caused by some combination of two factors: (1) a change in the rate-controlling mechanism to diffusion of reactants through semipermeable C–S–H product encasing the Ca_3SiO_5 particles,

G. Scherer—contributing editor

Manuscript No. 23996; Received November 19, 2007; approved January 29, 2008.
This work was supported by the Virtual Cement and Concrete Testing Laboratory Consortium and by the Partnership for High-Performance Concrete Technology program (HYPERCON) at the National Institute of Standards and Technology.
†Author to whom correspondence should be addressed. e-mail: bullard@nist.gov

‡Where it is convenient and not likely to cause confusion, conventional cement chemistry notation is used, i.e. C = CaO, S = SiO_2, and H = H_2O.

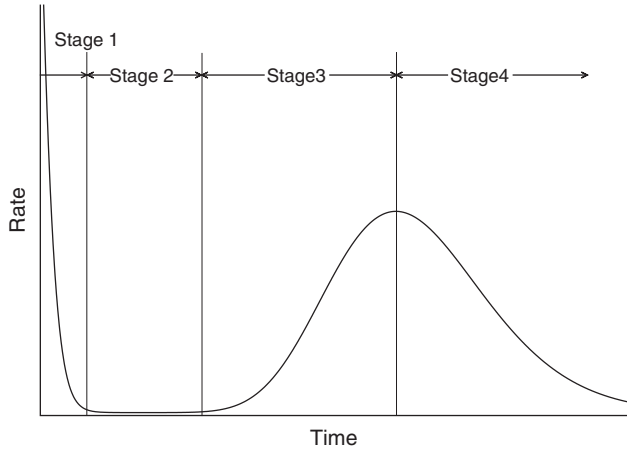

Fig. 1. Idealized rate of hydration of tricalcium silicate as a function of time.

and (2) decreasing surface area of this C–S–H product available for continued growth as the layers growing on each particle begin to impinge on each other.[2]

This general categorization into kinetic stages is further complicated by the experimental fact that both the duration of each stage of hydration and the rate of hydration during each stage depends on the chemical composition of the solution. The widespread use of retarding agents such as certain sugars,[30–32] and accelerating agents such as calcium chloride [22,32,33] take advantage of this situation.

Even in the absence of such intentional kinetic modifiers, the rate of hydration of Ca_3SiO_5 is sensitive to the concentration of calcium and hydroxyl ions in solution.[12,13,16,28] For example, Garrault and Nonat[12,13] conducted experiments on dilute stirred suspensions of Ca_3SiO_5 in which the molar concentration of calcium in solution was intentionally fixed either at 11 or 22 mmol/L by continuous sensing and modification of the solution. At 11 mmol/L, the system passed from Stages 1 to 3 with no induction period between them. However, Stage 3 lasted for only about 100 min, and afterward the hydration rate decreased rapidly in Stage 4. At the transition between Stages 3 and 4, the degree of hydration, or mass fraction of Ca_3SiO_5 consumed, was only about 0.04, and even after 300 min more the degree of hydration reached only 0.08. In contrast to this behavior, at 22 mmol/L Stage 1 was followed by a 100-min induction period before Stage 3 began. In addition, the transition from Stages 3 to 4 was delayed until about 5 h, at which time the degree of hydration was about 0.10. At 400 min of hydration, the degree of hydration was 0.15, nearly twice that of the 11 mmol/L system at the same time.

Elementary chemical kinetic theory indicates that the rate of any chemical reaction should increase when the concentrations of the reactants are increased. Therefore, if growth of a stoichiometric solid from solution is the rate-controlling step in a process, then increasing the concentration of all the reactants in solution should cause an immediate increase in growth rate. But the experiments just described indicate a much more complex dependence of reaction rate on calcium and hydroxyl ions. This unusual relationship between reaction rate and reactant concentrations is likely due, in part, to the variable composition and nanostructure of the C–S–H that nucleates and grows as the primary product of hydration.

C–S–H is a nanoporous, nonstoichiometric substance, and its composition is therefore sensitive to the composition of the surrounding solution. In fact, reported measurements of the calcium-to-silicon molar ratio (Ca/Si) of the C–S–H phase range from $\approx$0.8 to $\approx$2.0.[3,4,12,34] In addition, the density, morphology, pore structure, and pore size distribution of C–S–H also appear to depend on solution composition as well as other factors such as temperature. In consequence, the composition, nanostructure, and larger-scale morphology of C–S–H often vary significantly from point to point in the same system.[35]

Because of the variability in C–S–H composition and structure, the local composition and rates of nucleation and growth should depend on the concentrations of species that participate in the growth reaction. Assuming that C–S–H forms by precipitation of species from solution, a model reaction might be:

$$x\,Ca^{2+} + H_2SiO_4^{2-} + 2(x-1)\,OH^- + (y-x)\,H_2O \rightarrow C_x - S - H_y$$

Further assuming that the reaction is elementary, its order is equal to its molecularity and the rate equation is written as[§]

$$\frac{dC_xSH_y}{dt} = k(x,y)\left[Ca^{2+}\right]^x\left[H_2SiO_4^{2-}\right]\left[OH^-\right]^{2(x-1)}$$

where a quantity in square brackets denotes its molar concentration and $k(x, y)$ is the reaction rate constant, which may be dependent on stoichiometry. Therefore, the local rate of formation of C–S–H and its composition are expected to depend on the local solution composition. This situation is notably different from what one would expect for the precipitation of stoichiometric compounds like NaCl or Al_2O_3.

(2) Potential for Modeling

Computer modeling that combines chemical kinetics and microstructure development offers a unique opportunity to investigate the kinetics of cement hydration. Properly formulated, a three-dimensional (3-D) reaction-transport model can define and explore any number of hypothetical reaction paths and mechanisms. By comparing to experimental data, models should be able to identify the likely scenarios, and to estimate the kinetic parameters that govern the hydration process. Models of 3-D cement paste microstructure have been developed and applied for the past 20 years to clarify and quantify the role of various microstructure parameters of cement paste—water/solids ratio, cement particle size distribution, etc.—on the hydration and hardened properties of cement paste.[36–42] More recently, some mathematically sophisticated reaction-diffusion models also have been applied to the hydration of cement in two dimensions.[43–45] All of these models have successfully reproduced a number of features of cement hydration, and they have greatly increased our understanding of the general kinetic characteristics of such systems. However, the kinds of questions these models can answer is limited because they need to make a number of simplifying assumptions about the kinetics of nucleation and growth and because they require that the composition of C–S–H is fixed. In addition, all of these models use an *ad hoc* dependence of the dissolution rate of Ca_3SiO_5 on the amount of C–S–H formed, and so they cannot address questions about the underlying causes for that dependence.

In this paper, a detailed mechanistic description of the hydration of Ca_3SiO_5 is proposed and tested quantitatively using a recently developed numerical model called HydratiCA, that is well-suited to investigating fundamental aspects of kinetics. The model is described briefly in the next section, after which the proposed mechanism is laid out by enumerating phases that are assumed to form and the reaction sequence, rate constants, and other thermodynamic and kinetic parameters that describes the phase evolution. Simulation results using the model are presented that lend strong support to the proposed mechanism. Similarities are drawn between this mechanism and two leading theories of Ca_3SiO_5 hydration. An argument is made that key aspects of both theories are required to encompass the full range of kinetic and thermodynamic behavior of Ca_3SiO_5 hydration.

[§]In this paper, the chemical activity of pure water is assumed to be unity, which is a reasonable approximation, according to Henry's Law, as long as the mole fraction of water in solution is 0.9 or greater. In Ca_3SiO_5water systems, even when the calcium concentrations are at their maximum, the mole fraction of water in solution is never $<$0.99.

II. Model

HydratiCA is a computer model developed recently at the National Institute of Standards and Technology (NIST). Its algorithms are based on fundamental kinetic cellular automaton principles[46] and has an object-oriented structure that makes it extensible to a wide range of material systems. The computational details, validation, and examples of its use for simulating electrolyte diffusion, homogeneous and heterogeneous reactions, and nucleation phenomena are given elsewhere.[47,48] The material microstructure is discretized on a regular cubic lattice having a lattice spacing of λ. The initial cement particle and water microstructure is mapped onto this lattice by assigning a phase (e.g., Ca_3SiO_5 or water) to each lattice site. These materials are themselves finely discretized into quanta of concentration called *cells*; the number of cells of a given material at a particular lattice point determines its local concentration. Multiple materials may be present at any lattice site. The model simulates microstructure evolution iteratively by executing algorithms for transport and reactions over small time increments. Transport of mobile species is modeled by allowing each cell at a lattice site to execute a random walk to a neighboring site. The probability p of the walk depends on the effective diffusivity D of the mobile species at the site and the length of the time increment τ being considered,[47]

$$p = \frac{\tau D}{\lambda^2} \tag{1}$$

Similarly, probabilistic rules are formulated to simulate chemical reactions at a lattice site. The probability of the reaction occurring depends on the reaction rate constant and on the number of cells N_α of each reactant α that participates in the reaction. For example, the probability of occurrence of a homogeneous reaction is given by

$$p = k\xi^{\left(\sum_\alpha \nu_\alpha^{(r)}\right)-1}\tau \prod_\alpha \max\left[0, \prod_{m=1}^{\nu_\alpha^{(r)}} N_\alpha - m + 1\right] \tag{2}$$

where ξ is a constant parameter of the model that relates N_α to the molar concentration of species α, and $\nu_\alpha^r$is the molar stoichiometric coefficient of the reactant α participating in the reaction. Equation (2) strictly applies only to homogeneous reactions. The same kind of equation applies for heterogeneous reactions and nucleation events, however, although the length scaling is somewhat different.[48] The reaction is allowed if p exceeds a random number $q \in [0, 1]$ drawn from a uniform distribution. If the reaction occurs at a lattice site, then the number of cells of each reactant (product) is decremented (incremented) by the number required by the molar stoichiometric coefficients of the reaction. Reactions that can proceed at appreciable rates in both forward and reverse directions are modeled as two separate one-way reactions. Both Eqs. (1) and (2) have been shown to converge, in the limit $\tau, \lambda \to 0$ to the standard rate equations for diffusion and homogeneous reactions, respectively.[46]

By these algorithms, the microstructure evolves automatically as the model updates the types and numbers of cells at each lattice site during each time step. The model is quite general and can accommodate a wide range of simultaneously coupled reaction and transport phenomena if the correct kinds of input are provided. For example, to simulate the kinetics of coupled reactions according to transition state theory, one must supply the model with the absolute rate constant, activation enthalpy, nucleation energy barriers, and stoichiometric coefficients of each reaction. This information is sufficient for the model to capture the rate of reaction, the temperature dependence of the rate, and even the temperature dependence of the dynamic equilibrium state for reversible reactions.[48] In addition to these reaction parameters, several properties of each of the constituent substances are also required. For simple condensed phases like water and stoichiometric solids, the density, molar volume, and internal porosity must be supplied. For mobile ionic solute species, one must provide the electrical charge, the diffusion coefficient at infinite dilution, and the parameters needed to calculate the activity coefficients using the extended Debye-Hückel equation.[49] Values for many of these properties can be found in textbooks or other reference materials.[1,50–52] Finally, for solids that can exhibit a range of chemical compositions, the model simulates compositional and structural variability by microscopic coprecipitation of two stoichiometric end member phases that span the desired range of compositions and physical properties. Each end member is assigned values for all the properties just listed, and then the relative rates of formation of each end member at a lattice site determines the local composition of the phase. Compositional variability of C–S–H also has been modeled by stoichiometric end member phases in a recent thermodynamic model of hydration products.[49]

One of the strengths of this modeling approach is that it can be applied at a wide range of length scales. For a detailed analysis of C–S–H growth, a reasonable length scale would be $\lambda \approx 5$ nm to resolve the nanoscale porosity adequately. However, to simulate systems that also have important features at the micrometer length scale, such as cement paste, much larger values of λ are required for computational expedience. In such cases, a reasonable compromise is to assign an internal porosity and pore tortuosity to the C–S–H as additional intrinsic properties. This latter approach is the one taken in this study.

In the remainder of this paper, HydratiCA is applied to identify a plausible kinetic description of Ca_3SiO_5 hydration. A collection of coupled equations is identified and input along with values of the required material and reaction parameters listed earlier to model the hydration process on a simple system. The resulting simulations are compared with published experimental data on both the degree of hydration and solution chemistry as a function of time. A wide range of reaction sets and parameters were investigated in detail, guided by ideas from published theories of cement hydration kinetics.[2,5,12,13]. As described in the 'Discussion', most of these scenarios cannot be made even qualitatively consistent with published experimental data, and they will not be reported here. In fact, only the scenario that provided the best overall quantitative fit to two sets of published experimental data[13,53] will be considered in the following sections.

III. Materials and Reactions

Table I lists the materials included in these simulations with their assumed properties, and Table II shows all of the assumed reactions and relevant reaction parameters. In Table I the values of density (ρ) and molar volume (V_m) are taken from published data[1] except for the two assumed stable phases of C–S–H, denoted as C–S–H(I) and C–S–H(II). For these latter phases, values for density were chosen to be consistent with values reported by Jennings[54] for low-density and high-density forms of C–S–H, respectively, when the volume of the gel porosity is taken into account. The molar volumes of these phases were then inferred from their assumed stoichiometry. The values for the ionic

Table I. List of Materials and their Assumed Properties

Material/Ion	Formula	ρ (g/cm^3)	V_m (cm^3/mol)	Transport factor	D_o (10^{-9} m^2/s)
H_2O		1.00	18.07	1.0	3.0
Ca_3SiO_5		3.21	72.40	0.00	—
C–S–H(m)	$C_3S_2H_3$	1.75	100.0	0.01	—
C–S–H(I)	CSH_4	2.20	85.73	0.01	—
C–S–H(II)	C_2SH_5	1.85	161.2	0.75	—
$Ca(OH)_2$		2.24	33.08	0.00	—
Ca^{2+}	—	—	—	—	0.72
OH^-	—	—	—	—	5.28
$H_2SiO_4^{2-}$	—	—	—	—	0.70

Table II. List of Reactions and their Asumed Parameters

	Reaction	k_+ (298 K) (mol/(m^2·s))	k_- (298 K) (mol/(m^2·s))	ΔH_+ (kJ/mol)
1	$Ca_3SiO_5 + 3H_2O \rightleftharpoons 3Ca^{2+} + H_2SiO_4^{2-} + 4OH^-$	1.0×10^{-5}	3.3×10^{-4}	−137.6
2	$C-S-H(m) \rightleftharpoons 3Ca^{2+} + 2H_2SiO_4^{2-} + 2OH^-$	2.9×10^{-7}	4.0×10^{-10}	20.0
3	$C-S-H(I) \rightleftharpoons Ca^{2+} + H_2SiO_4^{2-} + 3H_2O$	1.6×10^{-7}	1.33	20.0
4	$C-S-H(II) \rightleftharpoons 2Ca^{2+} + H_2SiO_4^{2-} + 2OH^- + 3H_2O$	1.9×10^{-8}	1.32×10^{4}	20.0
5	$Ca(OH)_2 \rightleftharpoons Ca^{2+} + 2OH^-$	3.23×10^{-5}	0.7586	−17.06

The forward rate constant for the first reaction is assumed to vary inversely with (1) the volume function of metastable C−S−H(m) present at the lattice site, and (2) the molar concentrations of calcium and hydroxyl ions.

diffusion coefficients at infinite dilution in water are taken from published thermochemical databases.[52] The actual local diffusion coefficients are calculated from these by including corrections for the concentration dependence of the activity coefficients and the effect of electrostatic potential set up by the distribution of the ion charges.[47] The transport factor of each condensed phase in Table I is a dimensionless quantity that, when multiplied by the diffusion coefficient, gives the effective diffusion coefficient for ions diffusing through the internal porosity of the phase. Thus, for water in the absence of any solids, the transport factor is defined to be unity, while for solids with no internal porosity the transport factor is defined to be zero. For solids like C–S–H with nanoporosity that is not resolved on the scale of the model, a value between zero and one was chosen to estimate the presumably lower rate of transport through these phases.

Table II lists the five reactions that are assumed in the simulations. Of these, the calcium hydroxide/water reaction (reaction 5 in the table) has been studied most extensively. Values for the reverse rate constant (k_-) were inferred from experiments on the kinetics of calcium hydroxide crystal growth.[55] The forward rate constant (k_+) was calculated from the equilibrium constant K_{eq} using the relation $k_+/k_- \equiv K_{eq}$. The data for the other reactions are not as well established, but the forward rate constant for dissolution of Ca_3SiO_5 was estimated from measurements recently reported by Damidot *et al.*[16] In addition, for this dissolution reaction, the rate constant itself is asssumed to vary inversely with the local molar concentration of calcium and hydroxyl ions in solution, as reported by the same investigators.[16] Finally, the forward rate constant for dissolution of Ca_3SiO_5 also is assumed to vary inversely with the volume fraction of the metastable hydrate, C–S–H(m), to simulate its assumed low permeability and consequent ability to retard the dissolution of the underlying Ca_3SiO_5. This retarding influence of the metastable hydrate is critical for correctly describing the kinetics. In 'Discussion' section, a modeling strategy will be discussed that could enable an even more fundamental inquiry into this effect.

IV. Results

Using the assumed materials and reaction parameters in Tables I and II, the hydration experiments performed by Garrault and Nonat[13] were simulated. In the experiments, a dilute suspension of Ca_3SiO_5 particles, with median particle diameter of 15 μm, was prepared with a liquid/solid mass ratio of 50. The suspension was continually stirred at a constant temperature of 25°C and the calcium concentration of the solution was regulated by continuous monitoring of the electrical conductivity of the solution.

To model these experimental conditions, a Ca_3SiO_5/water system was mapped onto a lattice. The surface/volume ratio of the Ca_3SiO_5 was 0.29 μm^{-1}, which is consistent with irregularly shaped particles having a volume equal to a sphere with diameter of 15 μm.[56] Periodic boundary conditions were used at all boundaries of the lattice. The lattice itself was chosen to be $4 \times 4 \times 24$ lattice sites, with a lattice spacing of $\lambda = 1$ μm. This small lattice was chosen for computational efficiency and because larger-scale microstructural changes were not of direct interest in this study. The liquid/solid mass ratio (L/S) was chosen to be 0.5, 1.0, or 5.0.

The value of L/S = 50 used in the experiments is computationally impractical in this study, so the influence of L/S on the results was investigated first. Figure 2 shows the predicted degree of hydration as a function of time for systems with L/S = 0.5, 1.0, or 5.0. As indicated in the plot, the composition of the pore solution was not regulated. The figure clearly shows that the progression of hydration generally is more rapid at early times as L/S increases. In particular, the system with L/S = 5.0 seems not to exhibit an induction period, although its rate of hydration appears to decrease somewhat by 50 min before increasing again at about 100 min. This early-time behavior occurs because more dissolution of Ca_3SiO_5 is required before the greater volume of solution reaches a high enough calcium and silicate concentrations to significantly retard the dissolution of Ca_3SiO_5, either by the presence of calcium and hydroxyl ions in solution, as indicated by Damidot *et al.*,[16] or by the formation of the metastable C–S–H(m) phase, which is assumed to provide a low-permeability layer on the surface of the dissolving solid. At later times (>300 min), the hydration behavior seems to invert, with the system having L/S = 5.0 showing the least overall degree of hydration at later times.

All these differences disappear completely when the calcium concentration in solution is fixed at 22 mmol/L, as shown in Fig. 3. In this figure, the same three L/S ratios are tested, but the degree of hydration for all three systems collapses onto a single curve throughout the first 10 h. In these systems, the only solute that can vary in concentration is the silicate ion $H_2SiO_4^{2-}$, and its concentration will quickly be fixed by equilibrium with the metastable C–S–H(m) phase forming on the surface of Ca_3SiO_5.

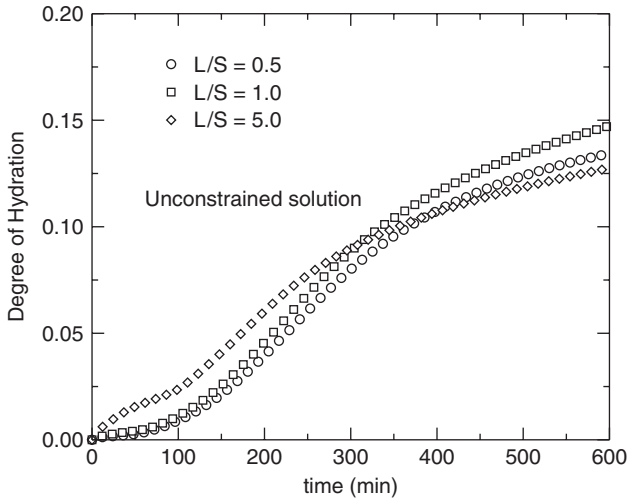

Fig. 2. Simulated degree of hydration as a function of time for suspensions of Ca_3SiO_5 with L/S = 0.5, 1, and 5. The solution is initially pure water and no constraints are placed on its composition. For the solid component, S/V = 0.29 μm^{-1}.

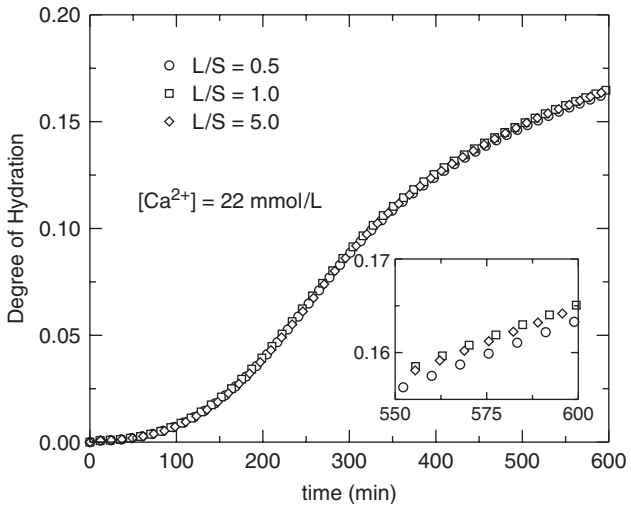

Fig. 3. Simulated degree of hydration as a function of time for suspensions of Ca_3SiO_5 with L/S = 0.5, 1, and 5, in which the calcium concentration of the solution was fixed at 22 mmol/L. For the solid, S/V = 0.29 μm^{-1}.

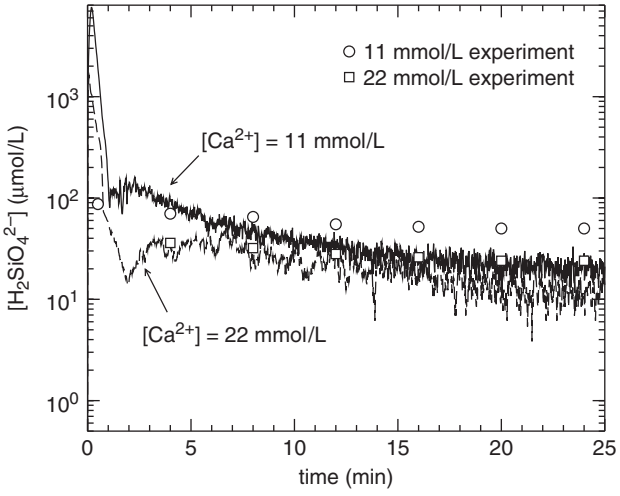

Fig. 5. Time-dependence of the concentration of silicate species in solution for the same system as in Fig. 4. The solid and dashed curves are the simulation predictions at calcium concentrations of 11 and 22 mmol/L, respectively. Discrete points are experimental measurements on suspensions with L/S = 50, published in Garrault and Nonat.[13]

Therefore, one expects—and the model predicts—that the hydration rate is independent of the L/S ratio when the calcium concentration of the solution is fixed. This result also supports claims made in previous papers that dilute suspensions are good models of cement pastes as long as the solution composition is regulated to mimic that found in pastes, i.e. nearly saturated with respect to calcium hydroxide.[11–13]

Having established that simulated paste at L/S = 0.5 is a good model of the dilute suspension used in the experiments in Garrault and Nonat,[13] provided that the calcium concentration in solution is fixed, we now compare the simulation predictions to the experimental data in that study. Figure 4 shows a comparison of the degree of hydration, that is, the fraction of Ca_3SiO_5 consumed, as a function of time when the calcium concentration was fixed at 11 or 22 mmol/L. The uncertainty in the experimental measurements, for example the accuracy with which the calcium concentration in solution was fixed, has not been reported. Absolute claims about the goodness of fit of the simulations therefore are not possible, but we can still make meaningful comparisons between the simulations and the data.

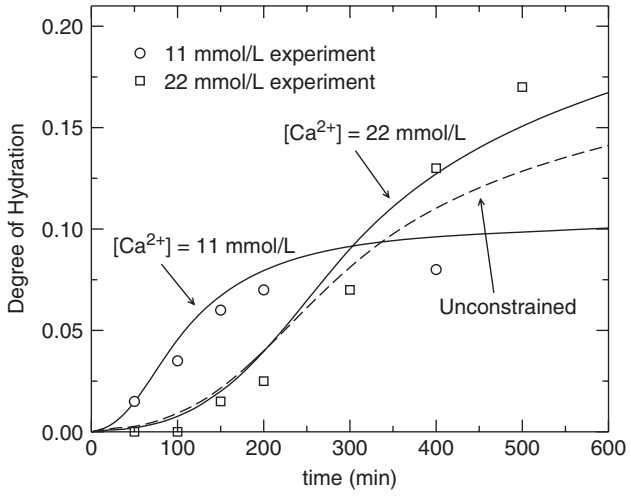

Fig. 4. Simulated hydration of a paste of tricalcium silicate with L/S = 0.5, and a ratio S/V = 0.29 μm^{-1} for the solid. The calcium concentration is fixed at 11 or 22 mmol/L. Solid curves are the simulation results, discrete points are experimental measurements on suspensions with L/S = 50, published in Garrault and Nonat,[13] and the dashed curve is the result of a simulation performed for hydration in initially pure water with no constraints on the evolving solution chemistry.

In the figure, the solid curves are the simulation results, and discrete points are experimental measurements reported in Garrault and Nonat.[13] The simulations capture the kinetic behavior both of the 11 and the 22 mmol/L system. In particular, when the calcium concentration is 11 mmol/L, the model correctly predicts both the absence of an induction period and the lower hydration rate at later ages relative to the system at 22 mmol/L calcium. The duration of the induction period at 22 mmol/L also is approximately correct. The uncertainty in the experimental measurements, for example the accuracy with which the calcium concentration in solution was fixed, has not been reported, so it is difficult to make any more detailed quantitative comment on the goodness of fit.

For the same simulated systems, the predicted and measured time dependence of silicate concentration are shown in Fig. 5. The predicted trends are qualitatively consistent with the experimental observations, although measured concentrations are two or three times greater than the predictions. It should be remembered that the measured silicate concentrations are very low in any case, on the order of a few tens of μmol/L with an unknown degree of certainty. In any case, the observed large decrease in silicate concentration in the first few minutes is captured by the model.

The dashed curve in Fig. 4 is the simulated degree of hydration in initially pure water with no constraints on the evolving solution chemistry. Comparison of this curve to experiment is not possible because the corresponding experiment was not performed in Garrault and Nonat[13] and, in any event, the invariance with L/S ratio would not be expected since the calcium concentration was not constrained. The main purpose of showing this simulation is to point out that the duration of the induction period and the initial acceleration between 100 and 200 min are predicted to be essentially the same in a paste as if the calcium concentration were fixed at 22 mmol/L. The rate of hydration at later ages, however, is predicted to be somewhat repressed compared with a paste having calcium concentration fixed at 22 mmol/L.

Differences in kinetic behavior at early ages between the systems with calcium concentrations at 11 and at 22 mmol/L can be traced to the different rates of growth of the various forms of C–S–H. Figure 6 plots the simulated growth of C–S–H(I) and C–S–H(II) in the two systems. When the calcium concentration is held at 11 mmol/L, a high density of C–S–H(I) nuclei form on the surface of Ca_3SiO_5 within seconds of wetting. The rate of nucleation is high because the system quickly becomes highly supersaturated with respect to C–S–H(I), with a saturation

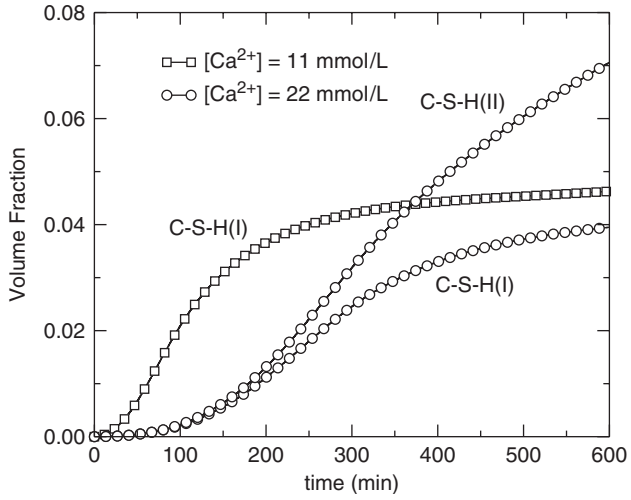

Fig. 6. Predicted growth kinetics of C–S–H(I) and C–S–H(II) for the same systems as in Fig. 4. The curve with open squares corresponds to the volume fraction of C–S–H(I) when the calcium concentration is fixed at 11 mmol/L, and the curves with open circles correspond to C–S–H(I) and C–S–H(II) when the calcium concentration is fixed at 22 mmol/L. For clarity, only one in every 700 points is displayed as a symbol, but the solid curve passes through all the intermediate points.

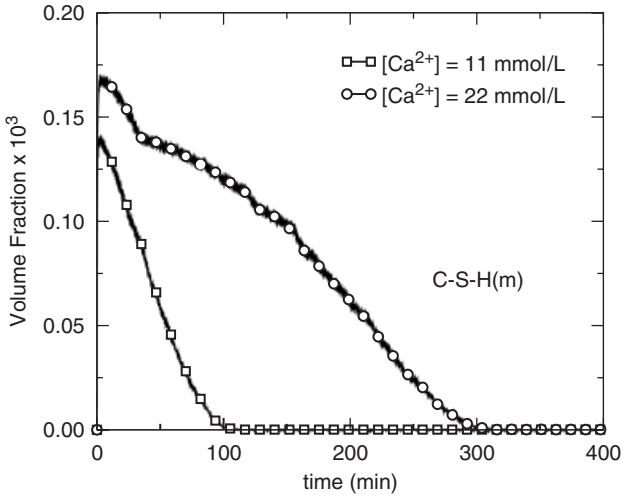

Fig. 7. Predicted time dependence of the volume fraction of C–S–H(m) for the same system as in Fig. 4. The curve with open squares corresponds to a fixed calcium concentration of 11 mmol/L, and the curve with open circles corresponds to a fixed calcium concentration of 22 mmol/L. For clarity, only one in every 700 points is displayed as a symbol.

index of almost 800 when nucleation occurs.[¶] On the other hand, the rate of C–S–H(II) nucleation is much lower because its saturation index is only about 300 when C–S–H(I) first nucleates. The nucleation rate is exponentially dependent on the saturation index,[48,57] so seemingly small differences in the saturation index correspond to large changes in nucleation rate. Because the density of C–S–H(II) nuclei, and therefore its surface area, is much lower than that of C–S–H(I), C–S–H(II) does not grow appreciably in this system. As the C–S–H(I) embryos grow and coalesce, they form a surface layer that resists molecular diffusion (transport factor = 0.01) and thereby slows the rate of dissolution of Ca_3SiO_5 at later ages, as shown in Fig. 4. The diminished rate of Ca_3SiO_5 dissolution allows the C–S–H(I) phase to establish near-equilibrium conditions with the solution, so its growth also slows considerably at later ages.

The rates of nucleation and growth of C–S–H(I) and C–S–H(II) are markedly different when the calcium concentration is 22 mmol/L. At this concentration, the saturation indices for C–S–H(I) and C–S–H(II) are about 200 and 600, respectively. Both forms nucleate at early times, but not as rapidly as C–S–H(I) does in the 11 mmol/L system. The combined growth rate of both forms of C–S–H is much less at early times than in the 11 mmol/L system because there is much less total surface area of the embryos.

The difference in initial combined growth rates of C–S–H(I) and C–S–H(II) is indirectly responsible for the observation that there is no induction period in the system with 11 mmol/L calcium in solution, but that there is a 100-min induction period in the 22 mmol/L system. Figure 7 shows a plot of the volume fraction of the metastable hydrate, C–S–H(m), as a function of time for both concentrations of calcium. The plot indicates that C–S–H(m) forms a surface layer within seconds after wetting occurs. However, the solubility of C–S–H(m) is greater than either C–S–H(I) or C–S–H(II), so when one or both of these phases nucleates and grows, the surrounding solution begins to become undersaturated with respect to C–S–H(m). Therefore, C–S–H(m) begins to dissolve, compromising its ability to protect the underlying Ca_3SiO_5 from dissolution. Because the growth of stable C–S–H is initially much faster in the 11 mmol/L system, the destruction of the C–S–H(m) layer occurs more quickly and no induction period is observed.

[¶]The solubility product K_{sp} for C–S–H(I) can be calculated from the rate constants given in Table 1 and the relation $k_+/k_- = K_{sp}$. The saturation index is defined as the ion activity product divided by K_{sp}.

With the kinetic predictions of the model in good agreement with the full set of experimental kinetic data in Garrault and Nonat,[13] we now may turn attention to whether the experimentally observed variations in C–S–H composition are also predicted by the model. Figure 8 shows the volume-averaged Ca/Si ratio of C–S–H plotted against time for the suspension at both fixed concentrations of calcium, i.e., 11 and 22 mmol/L. The data were obtained from the curves in Fig. 6 by multiplying the volume fraction of each phase of C–S–H by its assumed Ca/Si ratio, and then dividing by the combined volume fractions of all forms of C–S–H. The results in Fig. 8 are consistent with the measurements made on the same kinds of systems by Garrault and Nonat.[12] In particular, when the calcium concentration is 11 mmol/L, the average Ca/Si ratio of C–S–H is predicted by HydratiCA to rapidly approach unity, which is the assumed Ca/Si ratio of C–S–H(I). This is a consequence of the fact that nearly all of the C–S–H that forms in this system is Type I (see Fig. 6), and the result is consistent with experi-

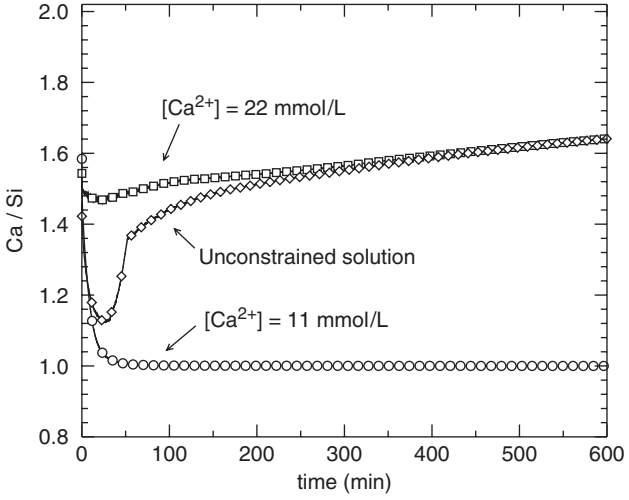

Fig. 8. Evolution of the volume-averaged Ca/Si ratio of C–S–H hydration product for the same system shown in Fig. 4. The calcium concentration is fixed at 11 mmol/L (○), fixed at 22 mmol/L (□), or allowed to vary naturally for dissolution into initially pure water (◇). Only one in every 400 points is displayed as a symbol, but the solid curve passes through all the intermediate points.

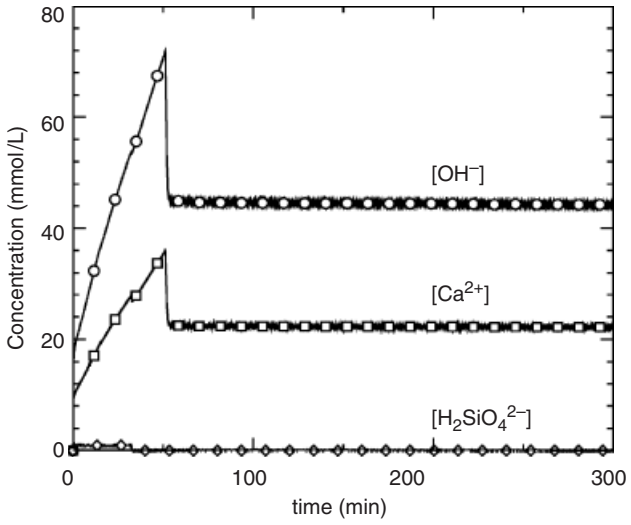

Fig. 9. Ion concentrations for the simulations when hydration is allowed to occur in initially pure water with no constraints on the solution composition.

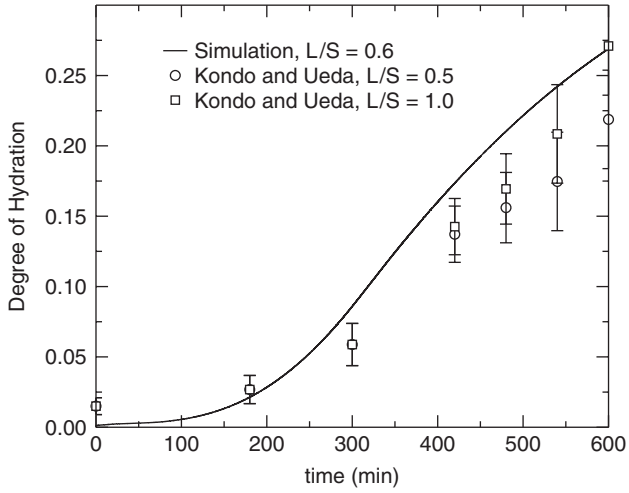

Fig. 10. Simulated degree of hydration as a function of time (solid curve) for a Ca_3SiO_5 paste with L/S = 0.59 and S/V = 0.86 μm^{-1} for the solid. The simulation was designed to approximate the experimental setup reported in Kondo and Ueda,[53] and the discrete points in the plot are the corresponding experimental data.

mentally measured value of $\approx 1.3 \pm 0.1$ reported for this system in.[12] In contrast, Fig. 6 shows that both stable types of C–S–H form at finite rates in the system having 22 mmol/L calcium in solution, although C–S–H(II) grows more rapidly after about 200 min. The consequence for C–S–H composition shown in Fig. 8 is that the Ca/Si ratio increases gradually from an average value of 1.5, reaching a value of 1.7 after 600 min of hydration. This prediction by HydratiCA also is reasonably consistent with experimental meaurements, Ca/Si $\approx 1.9 \pm 0.1$, for C–S–H grown in solutions with a calcium concentration of 22 mmol/L.[12]

A large number of studies have been made of the Ca/Si molar ratio of C–S–H formed in pastes of Ca_3SiO_5,[58,59] of $\beta-Ca_2SiO_4$,[60–62] and of ordinary Portland cement.[63–66] Most of these studies report values of 1.6 to 2.0 for the Ca/Si ratio. If the mechanisms used in the HydratiCA simulations are correct, then these studies imply that C–S–H(II) growth is favored relative to C–S–H(I) in these systems. To test this, a simulation was run on the same Ca_3SiO_5/water system with L/S = 0.5, except that the solution was free of constraints on its calcium concentration. The calcium, hydroxyl, and silicate concentrations in solution changed naturally as a net result of the reactions between Ca_3SiO_5 and water, as shown in Fig. 9. In this plot, both the calcium and hydroxyl concentrations are initially zero, rise almost immediately to approximately 10 and 18 mmol/L, respectively, and thereafter increase more slowly to maximum values of 36 and 71 mmol/L, respectively. At that point, portlandite ($Ca(OH)_2$) nucleates and rapidly depletes the solution of calcium and hydroxyl ions until a near-equilibrium state is reached at which $[Ca^{2+}] = 22$ mmol/L and $[OH^-] = 41$ mmol/L.

In Fig. 8, the middle curve with diamond symbols shows the predicted composition of C–S–H in this simulation. Initially, the Ca/Si ratio decreases sharply because the calcium concentration in solution is low. But as the calcium concentration continues to increase, growth of C–S–H(II) becomes increasingly favorable. After the time at which portlandite nucleates from solution, about 60 min, the solution is identical in composition to that in the earlier simulations when the calcium concentration was fixed at 22 mmol/L. In consequence, the Ca/Si ratio of C–S–H in the unconstrained suspension converges to the upper curve in Fig. 8. Therefore, these simulations provide a quantitative explanation, in terms of relative growth rates of C–S–H(I) and C–S–H(II), for the fact that the average Ca/Si ratio of C–S–H often lies between 1.6 and 2.0. Even further, the predicted lower value of Ca/Si at early ages for the dashed curve in Fig. 8 is supported by at least one study [58] in which the Ca/Si ratio was observed to be lower at very early ages than after several hours of hydration.

Up to this point, the kinetic predictions of the model have been verified by comparison to data measured on dilute stirred suspensions when the calcium concentration was fixed.[12,13] As a final check of the model, we now compare with experimental data on a Ca_3SiO_5 system reported by Kondo and Ueda.[53] In their experimental study almost 40 years ago, they measured the degree of hydration of Ca_3SiO_5 in pastes with L/S = 0.5 or 1.0. The pastes were made by mixing with pure water a powder having a narrow range of particle diameters, from 4 to 10 μm. The degree of hydration was measured by quantitative X-ray diffraction analysis of Ca_3SiO_5 at different times. The purity and crystal structure of the Ca_3SiO_5 powder used in the study was not reported.

A model paste with L/S = 0.6 was made by placing a single digitized spherical particle of Ca_3SiO_5, with surface-volume ratio S/V = 0.86 μm^{-1}, in pure water. The chosen value of S/V is equal to that of a smooth spherical particle with diameter of 8 μm, which is in the middle of the particle size range used in Kondo and Ueda.[53] Figure 10 compares the simulated degree of hydration to the measured degrees of hydration of pastes with L/S = 0.5 and 1.0, estimated from Fig. 1 in Kondo and Ueda.[53] Error bars on the experimental data reflect only the uncertainty in reading the values from that logarithmic plot; the actual uncertainty in the experimental data was not reported in Kondo and Ueda.[53] All the parameters for materials and reactions were the same as in the previous simulations in this section. The plot indicates that the predicted induction period is consistent with experimental observation on both pastes. However, after the induction period the hydration of the simulated paste accelerates more rapidly than experimentally observed in either paste. The simulated degree of hydration is modestly but consistently greater than the measured values between 5 and 9 h. The reason for this relatively small disagreement is unclear, although differences in impurity levels, and especially in crystal structure, of the initial Ca_3SiO_5 powder might cause deviations in hydration rates at least as great as those observed here.

V. Discussion

A large number of possible sets of reactions, rate constants, and material parameters were systematically explored before arriving at the values given in Table I and II. This was necessary because, as stated earlier, there is no universal agreement on the reaction paths and rate-controlling steps that govern Ca_3SiO_5 hydration. For example, there is some debate in the literature over whether a metastable hydrate phase forms on the surface of

Ca_3SiO_5 at early ages and, if it does, what the implications are for hydration kinetics.[4,67,68] In the absence of a consensus about the mechanism, HydratiCA was used as a kind of experimental tool for exploring the plausibility of various mechanisms. The results indicate that the most plausible model for the hydration kinetics is a synthesis of the two most prominent models that have been put forward in recent years.

In the following discussion, we will operate from the point of view that any comprehensive model of the hydration kinetics of Ca_3SiO_5 must be able to predict and explain (1) the extremely rapid decrease in reaction rate during the first minutes after wetting, (2) the existence of an induction period in which little reaction occurs and the solution maintains a nearly constant composition, and (3) the eventual acceleration of the hydration rate in a manner reminiscent of an autocatalytic process. The experimental data reported by Garrault and Nonat[12,13] are extremely valuable because, by fixing the concentration of calcium in the solution, they reduce the number of degrees of freedom of the solution composition to just one: the concentration of silicate ions. Such data make a comparison of the solution composition and the kinetics of hydration much less ambiguous than previously was possible.

For simplicity, we will refer to the two leading theories of Ca_3SiO_5 hydration as the *equilibrium theory* and the *steady-state theory* of the induction period. They both assume that dissolution of Ca_3SiO_5 in pure water is congruent, extremely rapid, and always far from equilibrium. The models differ principally in their explanation of why the induction period exists and how the acceleration period begins. To review, the equilibrium theory[2] assumes that a C–S–H(m) layer forms within seconds of wetting and represents a semipermeable barrier that reduces the dissolution rate of Ca_3SiO_5 by two or three orders of magnitude. This layer, although quite thin, is a true phase with well-defined thermodynamic properties, including an equilibrium constant in water. In particular, because the dissolution of Ca_3SiO_5 is slow after this layer forms, C–S–H(m) can establish equilibrium with the solution, which explains the nearly constant composition of the solution during the induction period. The equilibrium theory further assumes that C–S–H(m) is metastable with respect to another stable form of C–S–H. When the stable form of C–S–H eventually precipitates, it destabilizes the C–S–H(m) layer. Immediately after it nucleates, the growth of stable C–S–H is assumed to proceed slowly because of the low surface area of the growing embryos, but the surface area increases with continued growth, and the C–S–H growth rate increases in proportion to the surface area available for growth. Dissolution of the C–S–H(m) layer accelerates as the growth rate of stable C–S–H accelerates. In consequence, the dissolution rate, i.e. hydration rate, of Ca_3SiO_5 accelerates during this period. Thus the acceleration period is mediated by a rate-controlling step of growth of stable C–S–H. However, the equilibrium theory, as currently formulated in the literature, does not predict the wide range of hydration rates that are now known to occur when the solution composition is adjusted.[12,13]

The steady-state theory[10,12,67] has perhaps been described most clearly by Garrault and Nonat,[13] where they used it to interpret their experimental data, the same data used in the previous section for most of the tests of HydratiCA. According to this theory, a metastable C–S–H(m) phase is not required to explain the kinetics of Ca_3SiO_5 hydration. Instead, the theory assumes that heterogeneous nucleation of a stable C–S–H on Ca_3SiO_5 surfaces happens almost immediately after wetting. This nucleation burst is used to explain the observed maximum in silicate concentration at early ages (Fig. 5). Furthermore, the nucleation rate depends on the calcium concentration. At low calcium concentrations, a large number of surface nuclei are assumed to form per unit area of Ca_3SiO_5 surface. These nuclei grow along the surface and coalesce to form a continuous layer at early ages that restricts the diffusion of water and thereby represses hydration at later ages. At higher calcium concentrations, the initial density of C–S–H nuclei on the Ca_3SiO_5 surfaces is lower, and coalescence into a continuous layer takes longer, not only because there are fewer nuclei per unit area, but also because they are assumed to grow more rapidly in the direction normal to the Ca_3SiO_5 surface. At any calcium concentration, though, the composition of the solution changes very slowly during this initial growth period, and this is assumed to be due to a *steady state* between dissolution of Ca_3SiO_5 on the one hand and growth of C–S–H on the other, the rates of these two processes being nearly the same and causing little net change in the solution composition. But even after nucleation, a large fraction of the Ca_3SiO_5 surface is exposed to solution. Therefore, the nucleation and growth rate of C–S–H within the first few minutes after wetting would have to be at least as great as the initial dissolution rate of Ca_3SiO_5 to cause a maximum in the silicate concentration and a steady-state condition afterward (Fig. 5). Such high growth rates of C–S–H are not indicated by direct observation of flat Ca_3SiO_5 surfaces in water using atomic force microscopy,[13] nor by microscopic obervations of Ca_3SiO_5 particles in dilute suspensions by soft X-ray transmission microscopy.[22] To reconcile the observed low growth rate of C–S–H to the steady-state theory, it is assumed that the dissolution rate of Ca_3SiO_5 decreases sharply with increasing concentrations of calcium and hydroxyl ions, to about the initial rate of growth of C–S–H, due to preferential adsorption and deactivation of dissolution sites. There is some experimental evidence supporting this latter assumption,[16] although the magnitude of the effect seems to be uncertain.

Simulation results obtained by HydratiCA support most aspects of this latter theory. First, as already noted, the simulations predict that the density of C–S–H(I) surface nuclei is greater in the 11 mmol/L than the combined density of C–S–H(I) and C–S–H(II) nuclei in the 22 mmol/L system, as required by steady-state theory.[13] Second, the variation in the average Ca/Si molar ratio of C–S–H predicted by the simulations is also an integral part of the steady-state theory to explain the quantitative differences between the maximum values of silicates in solution at different calcium concentrations[13] and the calculated rates of nucleation of C–S–H.[12]

With regard to the steady-state theory's assumed differences in the nanoscale anisotropy in growth of C–S–H at different calcium concentrations, these simulations did not incorporate growth anisotropy of surface nuclei because the length scale of the simulations was too large to resolve it. Nevertheless, the differences in transport factor of C–S–H(I) and C–S–H(II) used in the simulations could be interpreted to support the hypothesis that the growth anisotropy is different for these two forms. Recall that the transport factor is a coarse-grained parameter that describes the relative ease with which mobile species can be transported through a material. A larger transport factor for C–S–H(II) could be caused by a difference in nanoscale porosity of a uniform layer of the material, but it could also be caused by relatively large, open pore channels between C–S–H domains that grow more readily in the direction normal to the Ca_3SiO_5 surface than toward each other along the surface. At the length scale used in these simulations, it is not possible to differentiate between these two possibilities.

There is one crucial point, however, at which the theoretical model tested here by HydratiCA, and shown to be consistent with the experimental data, cannot be reconciled to the steady-state theory, and this point is the necessity and role of the metastable C–S–H(m) phase which is the distinguishing aspect of the equilibrium theory. Many trial simulations were made with HydratiCA to try to make the kinetics of Ca_3SiO_5 hydration consistent with the experiments without the formation of a C–S–H(m) phase. In these trials, only the differences in concentrations of calcium and hydroxyl ions were allowed to influence the rate constant for Ca_3SiO_5 dissolution. That is, the rate constant for dissolution of Ca_3SiO_5 was made to vary inversely with both the local calcium concentration and the hydroxyl concentration, evaluated at each lattice site eligible for dissolution. Different empirical inverse relationships were tested, including linear and exponential decreases in the rate constant with concentrations of calcium and hydroxyl ions. But in all

such trials, this mechanism alone was unable to generate the required extremes in the dissolution rate of Ca_3SiO_5. If the calcium and hydroxyl concentrations are fixed throughout hydration, as they were in the experiments of Garrault and Nonat,[12,13] then the influence on dissolution rate of adsorption of these species should be *constant* during any given experiment. However, the experimental data clearly show a very low rate of dissolution during the induction period—which also is required by the steady-state theory to maintain steady state with the slowly growing C–S–H domains—followed by a much greater dissolution rate during the acceleration period a couple hours later. Furthermore, the very early-age changes in silicate concentration indicate that the Ca_3SiO_5 dissolution rate also is extremely high immediately upon wetting. These observations are inconsistent with the assumption that calcium or hydroxyl concentration alone determines the dissolution rate of exposed Ca_3SiO_5 surface area.

Since these simulations suggest that the formation and stability of C–S–H(m) is important for determining the early-age rates of hydration, it would be instructive to model the C–S–H(m) layer in more detail by applying the model at much smaller length scales near the Ca_3SiO_5 surface. This would allow a more direct determination of growth rate constant and transport factor of C–S–H(m) that would be required to account for its retarding influences on Ca_3SiO_5 dissolution. In addition, the present study has identified two compositional variants of stable C–S–H, each of which has a different coarse-grained transport factor that approximates the tortuosity of its nanoscale porosity. If this is basically correct, as published experiments seem to indicate,[12,35] then the same model could be used, again at much smaller length scales, as part of an investigation of the differences in structure between these variants. At the moment, it is unclear why differences in C–S–H composition are related to differences in porosity structure at scales of 10 nm to 1 μm, particularly since C–S–H growth seems to occur by aggregation of fundamental building units with dimensions of about 5 nm.[34] New physical insight might be gained about this process by combining molecular-scale models with the kind of modeling reported here.

VI. Summary

This study illustrates the considerable potential for using fundamental computer simulations as a kind of experimental apparatus for testing kinetic models of aqueous mineral systems, and for developing new ones where necessary. These kinds of simulations can provide new insights on how kinetic mechanisms operating at a microscopic scale can influence experimental observations of kinetics and chemistry on a macroscopic scale.

In this first application to a cementitious material system, HydratiCA has identified what we now consider, in light of available experimental data, to be the only plausible comprehensive kinetic model for the Ca_3SiO_5/water system. This kinetic description incorporates the composition-dependent nucleation and growth of C–S–H on the surface of Ca_3SiO_5 to account for observed variations in the length of the induction period. However, the induction period itself seems to be best characterized by near equilibrium between the solution and a thin layer of a metastable hydrate phase that forms on Ca_3SiO_5 upon wetting and that provides a kinetic barrier against further rapid hydration. Nucleation of more stable C–S–H in the metastable layer also occurs at early times, and its growth destabilizes the metastable layer by a through-solution mechanism and reinitiates dissolution of Ca_3SiO_5. Therefore, once stable embryos of stable C–S–H are established, its growth controls the rate of hydration during the induction and acceleration periods.

This description of the kinetics draws on features from each of the two leading theories that have appeared in the literature, what have been called here the equilibrium theory and the steady-state theory. The unification of these two theories, which until this study seemed unlikely to occur, is fitting because they both have had considerable success in explaining different aspects of early-age hydration of Ca_3SiO_5.

Acknowledgments

The author is indebted to Denis Damidot, Ellis Gartner, Sandrine Garrault, Hamlin Jennings, André Nonat, and Jeff Thomas for their insightful comments and helpful discussions. Ken Snyder and Vijay Gupta provided thoughtful critiques of the paper.

References

[1]H. F. W. Taylor, *Cement Chemistry*, 2nd edition, Thomas Telford, London, 1997.
[2]E. M. Gartner and J. M. Gaidis, "Hydration Mechanisms, I"; pp. 95–125 in *Materials Science of Concrete*, Vol. 1, Edited by J. Skalny. American Ceramic Society, Westerville, OH, 1989.
[3]P. W. Brown, E. Franz, G. Frohnsdorff, and H. F. W. Taylor, "Analyses of the Aqueous Phase During Early C_3S Hydration," *Cem. Concr. Res.*, **14**, 257–62 (1984).
[4]H. M. Jennings, "Aqueous Solubility Relationships for Two Types of Calcium Silicate Hydrate," *J. Am. Ceram. Soc.*, **69** [8] 618 (1986).
[5]E. M. Gartner and H. M. Jennings, "Thermodynamics of Calcium Silicate Hydrates and their Solutions," *J. Am. Ceram. Soc.*, **80** [10] 743–9 (1987).
[6]P. W. Brown, "Phase Equilibria and Cement Hydration"; pp. 73–93 in *Materials Science of Concrete*, Vol. 1, Edited by J. Skalny. American Ceramic Society, Westerville, OH, 1989.
[7]C. L. Dickson, D. R. M. Brew, and F. P. Glasser, "Solubilities of $CaO–SiO_2–H_2O$ Phases at 25°, 55°, and 85°C," *Adv. Cem. Res.*, **16** [1] 35–43 (2004).
[8]J. J. Chen, J. J. Thomas, H. F. W. Taylor, and H. M. Jennings, "Solubility and Structure of Calcium Silicate Hydrate," *Cem. Concr. Res.*, **34**, 1499–519 (2004).
[9]P. Barret and D. Ménétrier, "Filter Dissolution of C_3S as a Function of the Lime Concentration in a Limited Amount of Lime Water," *Cem. Concr. Res.*, **10**, 521–34 (1980).
[10]P. Barret, D. Ménétrier, and D. Bertrandie, "Mechanism of C_3S Dissolution and Problem of the Congruency in the Very Initial Period and Later On," *Cem. Concr. Res.*, **13**, 728–38 (1983).
[11]D. Damidot, A. Nonat, and P. Barret, "Kinetics of Tricalcium Silicate Hydration in Diluted Suspensions by Microcalorimetric Measurements," *J. Am. Ceram. Soc.*, **73** [11] 3319–22 (1990).
[12]S. Garrault-Gauffinet and A. Nonat, "Experimental Investigation of Calcium Silicate Hydrate (C–S–H) Nucleation," *J. Cryst. Growth*, **200**, 565–74 (1999).
[13]S. Garrault and A. Nonat, "Hydrated Layer Formation on Tricalcium and Dicalcium Silicate Surfaces: Experimental Study and Numerical Simulations," *Langmuir*, **17**, 8131–8 (2001).
[14]R. A. Livingston, J. S. Schweitzer, C. Rolfs, H. W. Becker, and S. Kubsky, "Characterization of the Induction Period in Tricalcium Silicate Hydration by Nuclear Resonance Reaction Analysis," *J. Mater. Res.*, **16** [3] 687–93 (2001).
[15]A. J. Allen, J. C. McLaughlin, D. A. Neumann, and R. A. Livingston, "In situ Quasi-Elastic Scattering Characterization of Particle Size Effects on the Hydration of Tricalcium Silicate," *J. Mater. Res.*, **19** [11] 3242–54 (2004).
[16]D. Damidot, F. Bellmann, B. Möser, and T. Sovoidnich, "Calculation of the Dissolution Rate of Tricalcium Silicate in Several Electrolyte Compositions," *Cement-Wapno-Beton*, **12/74** [2] 57–67 (2007).
[17]R. Kondo and M. Daimon, "Early Hydration of Tricalcium Silicate: A Solid Reaction with Induction and Acceleration Periods," *J. Am. Ceram. Soc.*, **52** [9] 502–8 (1969).
[18]D. Ménétrier, I. Jawed, T. S. Sun, and J. Skalny, "ESCA and SEM Studies on Early C_3S Hydration," *Cem. Concr. Res.*, **9**, 473–82 (1979).
[19]A. Nonat, "Interactions between Chemical Evolution (Hydration) and Physical Evolution (Setting) in the Case of Tricalcium Silicate," *Mater. Struct.*, **27**, 187–95 (1994).
[20]M. C. G. Juenger and H. M. Jennings, "New Insights into the Effects of Sugar on the Hydration and Microstructure of Cement Pastes," *Cem. Concr. Res.*, **32**, 393–9 (2002).
[21]S. Garrault, E. Finot, E. Lesniewska, and A. Nonat, "Study of C–S–H Growth on C_3S Surface During its Early Hydration," *Mater. Struct.*, **38**, 435–42 (2005).
[22]M. C. G. Juenger, P. J. M. Monteiro, E. M. Gartner, and G. P. Denbeaux, "A Soft X-Ray Microscope Investigation into the Effects of Calcium Chloride on Tricalcium Silicate Hydration," *Cem. Concr. Res.*, **35** [1] 19–25 (2005).
[23]D. A. Silva and P. J. M. Monteiro, "Hydration Evolution of C_3S-EVA Composites Analyzed by Soft X-Ray Microscopy," *Cem. Concr. Res.*, **35**, 351–7 (2005).
[24]H. F. W. Taylor, P. Barret, P. W. Brown, D. D. Double, G. Frohnsdorff, V. Johansen, D. Ménétrier-Sorrentino, I. Odler, L. J. Parrott, J. M. Pommersheim, M. Regourd, and J. F. Young, "The Hydration of Tricalcium Silicate," *Mater. Struct.*, **17**, 457–68 (1984).
[25]H. N. Stein, "Thermodynamic Considerations on the Hydration Mechanisms of Ca_3SiO_5 and $Ca_3Al_2O_6$," *Cem. Concr. Res.*, **2** [2] 167–77 (1972).
[26]H. N. Stein and J. M. Stevels, "Influence of Silica on the Hydration of 3 CaO,SiO_2," *J. Appl. Chem.*, **14**, 338–46 (1964).
[27]H. M. Jennings and P. L. Pratt, "An Experimental Argument for the Existence of a Protective Membrane Surrounding Portland Cement During the Induction Period," *Cem. Concr. Res.*, **9**, 501–6 (1979).
[28]A. Nonat and D. Damidot "Hydratation des ciments et stabilité chimique des hydrates, mécanismes d'évolution physico-chimique du béton dans son environnement," ATILH Publication , personal commnunication, August 2006.

[29]M. Avrami, "Granulation, Phase Change, and Microstruture: Kinetics of Phase Change. III," *J. Chem. Phys*., **9**, 177–84 (1941).
[30]J. F. Young, "A Review of the Mechanisms of Set-Retardation in Portland Cement Pastes Containing Organic Admixtures," *Cem. Concr. Res*., **2** [5] 415–33 (1972).
[31]M. C. G. Juenger and H. M. Jennings, "Effects of High Alkalinity on Cement Pastes," *ACI Mater. J*., **98** [3] 251–5 (2001).
[32]V. K. Peterson and M. C. G. Juenger, "Hydration of Tricalcium Silicate: Effects of $CaCl_2$ and Sucrose on Reaction Kinetics and Product Formation," *Chem. Mater*., **18**, 5798–804 (2006).
[33]K. Murakami and H. Tanaka "Contribution of Calcium Thiosulphate to the Acceleration of the Hydration of Portland Cement and Comparison with Other Soluble Inorganic Salts," in *Proceedings of the Fifth International Symposium on the Chemistry of Cement, Part II. Hydration of Cements*, volume 2, pp. 422–436, 1968.
[34]A. J. Allen, J. J. Thomas, and H. M. Jennings, "Composition and Density of Nanoscale Calcium–Silicate–Hydrate in Cement," *Nat. Mater*., **6**, 311–6 (2007).
[35]I. G. Richardson, "Tobermorite/Jennite- and Tobermorite/Calcium Hydroxide-Based Models for the Structure of C–S–H: Applicability to Hardened Pastes of Tricalcium Silicate, β-Dicalcium Silicate, Portland Cement, and Blends of Portland Cement with Blast-Furnace Slag, Metakaolin, or Silica Fume," *Cem. Concr. Res*., **34**, 1733–77 (2004).
[36]H. M. Jennings and S. K. Johnson, "Simulation of Microstructure Development during the Hydration of a Cement Compound," *J. Am. Ceram. Soc*., **69** [11] 790–5 (1986).
[37]K. van Breugel, *Simulation of Hydration and Formation of Structure in Hardening Cement-Based Materials*, PhD dissertation, Delft University of Technology, Delft, The Netherlands (1991).
[38]D. P. Bentz, E. Schlangen, and E. J. Garboczi, "Computer Simulation of Interfacial Zone Microstructure and its Effect on the Properties of Cement-Based Composites"; pp. 155–200 in *Materials Science of Concrete IV*, Edited by J. Skalny, and S. Mindess. American Ceramic Society, Westerville, OH, 1995.
[39]K. van Breugel, "Numerical Simulation of Hydration and Microstructural Development in Hardening Cement-Based Materials. (I) Theory," *Cem. Concr. Res*., **25** [2] 319–31 (1995).
[40]D. P. Bentz, "Three-Dimensional Computer Simulation of Cement Hydration and Microstructure Development," *J. Am. Ceram. Soc*., **80** [1] 3–21 (1997).
[41]E. J. Garboczi and D. P. Bentz, "The Effect of Statistical Fluctuation, Finite Size Error, and Digital Resolution on the Phase Percolation and Transport Properties of the NIST Cement Hydration Model," *Cem. Concr. Res*., **31**, 1501–4 (2001).
[42]C. Pignat, P. Navi, and K. Scrivener, "Simulation of Cement Paste Microstructure Hydration, Pore Space Characterization and Permeability Determination," *Mater. Struct*., **38**, 459–66 (2005).
[43]F. Tzschichholz, H. J. Herrmann, and H. Zanni, "Reaction-Diffusion Model for the Hydration and Setting of Cement," *Phys. Rev. E*, **53** [3] 2629–37 (1996).
[44]F. Tzschichholz and H. Zanni, "Global Hydration Kinetics of Tricalcium Silicate Cement," *Phys. Rev. E*, **64** [1] 016115 (2001).
[45]S. J. Preece, J. Billingham, and A. C. King, "On the Initial Stages of Cement Hydration," *J. Eng. Mech*., **40** [1] 43–58 (2001).
[46]T. Karapiperis and B. Blankleider, "Cellular Automaton Model of Reaction-Transport Processes," *Physica D*., **78**, 30–64 (1994).
[47]J. W. Bullard, "Approximate Rate Constants for Nonideal Diffusion and their Application in a Stochastic Model," *J. Phys. Chem. A*., **111** [11] 2084–92 (2007).
[48]J. W. Bullard, "A Three-Dimensional Microstructural Model of Reactions and Transport in Aqueous Mineral Systems," *Modell. Simulat. Mater. Sci. Eng*., **15**, 711–38 (2007).
[49]B. Lothenbach and F. Winnefeld, "Thermodynamic Modelling of the Hydration of Portland Cement," *Cem. Concr. Res*., **36**, 209–26 (2006).
[50]D. Langmuir, *Aqueous Environmental Geochemistry*. Prentice-Hall, London, UK, 1997.
[51]D. L. Parkhurst "User's Guide to PHREEQC—A Computer Program for Speciation Reaction-Path, Advective-Transport, and Geochemical Calculations," *Water-Resources Investigations Report 95-4227*, U.S. Geological Survey (1995).
[52]R. Mills and V. M. M. Lobo, *Self-Diffusion in Electrolyte Solutions*. Elsevier, Amsterdam, 1989.
[53]R. Kondo and S. Ueda "Kinetics and Mechanisms of the Hydration of Cements," in *Proceedings of the Fifth International Symposium on the Chemistry of Cement, Part II. Hydration of Cements*, volume 2, pp. 203–212, 1968.
[54]H. M. Jennings, "A Model for the Microstructure of Calcium Silicate Hydrate in Cement Paste," *Cem. Concr. Res*., **30**, 101–16 (2000).
[55]M. E. Tadros, J. Skalny, and R. S. Kalyoncu, "Kinetics of Calcium Hydroxide Crystal Growth from Solution," *J. Colloid Interface Sci*., **55** [1] 20–4 (1976).
[56]E. J. Garboczi and J. W. Bullard, "Shape Analysis of a Reference Cement," *Cem. Concr. Res*., **34**, 1933–7 (2004).
[57]D. Kaschiev and G. M. van Rosmalen, "Review: Nucleation in Solutions Revisited," *Crys. Res. Technol*., **38** [7–8] 555–74 (2003).
[58]I. Odler and H. Dörr, "Early Hydration of Tricalcium Silicate. 1. Kinetics of the Hydration Process and the Stoichiometry of the Hydration Products," *Cem. Concr. Res*., **9** [2] 239–48 (1979).
[59]L. J. Parrott and D. C. Killoh, "Prediction of Cement Hydration," *Br. Ceram. Proc*., **35**, 41–53 (1984).
[60]K. Fujii and W. Kondo, "Rate and Mechanism of Hydration of β-Dicalcium Silicate," *J. Am. Ceram. Soc*., **62** [3–4] 161–7 (1979).
[61]D. L. Kantro and C. H. Weise, "Hydration of Various β-Dicalcium Silicate Preparations," *J. Am. Ceram. Soc*., **62** [11–12] 621–6 (1979).
[62]S. Shibata, K. Kishi, K. Asaga, M. Daimon, and P. R. Shrestha, "Preparation and Hydration of β-Dicalcium Silicate without Stabilizer," *Cem. Concr. Res*., **14** [3] 323–8 (1979).
[63]D. L. Rayment and A. J. Majumdar, "The Composition of the C–S–H Phases in Portland-Cement Pastes," *Cem. Concr. Res*., **12** [6] 753–64 (1982).
[64]P. L. Rayment, "The Effect of Pulverized-Fuel Ash on the C-S Molar Ratio and Alkali Content of Calcium Silicate Hydrates in Cement," *Cem. Concr. Res*., **12** [2] 133–40 (1982).
[65]H. F. W. Taylor and D. E. Newbury, "An Electron-Microprobe Study of a Mature Cement Paste," *Cem. Concr. Res*., **14** [4] 565–73 (1984).
[66]D. L. Rayment, "The Electron-Microprobe Analysis of the C–S–H Phases in a 136-Year-Old Cement Paste," *Cem. Concr. Res*., **16** [3] 341–4 (1986).
[67]P. Barret and D. Bertrandie, "Comment on 'Aqueous Solubility Relationships for Two Types of Calcium Silicate Hydrate'," *J. Am. Ceram. Soc*., **71** [2] C–113–5 (1988).
[68]H. M. Jennings, "Reply," *J. Am. Ceram. Soc*., **71** [2] C–115–6 (1988). □